

A study on high temperature corrosion of 20G in precipitated sodium sulfate

Jihui Wu¹, Bing Bai², Xuezhao Zhao¹, Naifeng Zhang¹, Chao Chen¹, Lei Deng², Defu Che^{2*}

¹ Steam Injection Services, Shengli Oilfield Company, Sinopec, Dongying 257001, China

² State Key Laboratory of Multiphase Flow in Power Engineering, School of Energy and Power Engineering, Xi'an Jiaotong University, Xi'an 710049, China)

ABSTRACT

The safety and efficiency of boilers are tightly related to the performance of boiler tube. 20G steel is widely used in the manufacturing of boiler tube. The corrosion behaviors of 20G exposed in precipitated sodium sulfate under high temperature/ pressure were investigated experimentally. Samples are placed in a setup for corrosion and subsequently analyzed by scanning electron microscope, energy dispersive spectroscopy (SEM / EDS) analysis and X-ray diffraction (XRD). The results indicate that the mass fraction of Fe elements on the surface decreases with time from 86.50% ($t = 24$ h) to 75.75% ($t = 72$ h). In the range of experiment temperature, higher temperature has positive effect on the formation of crystal structures.

KEYWORDS: boiler tube, water side corrosion, high temperature, sodium sulfate

NONMENCLATURE

<i>Abbreviations</i>	
h	Hour(s)
<i>Symbols</i>	
T	Temperature
t	Heating time

1. INTRODUCTION

The performance of boiler tubes is of great significance in energy applications as boilers are widely used in lots of industry processes. Corrosion behavior of boiler tubes has an effect on the tube performance and it also plays an important role in boiler operation. Steel

corrosion results in lots of safety problems every year around the world^[1]. In boiler, steel corrosion on water side is one of the main inducements leading to heat transfer deterioration and material failure as the oxide films formed on the working medium side could lead to major failures and consequently to reduced boiler availability. There are many kinds of steels used in boiler manufacturing. To figure out the behavior of water side corrosion, C. Yuan et al^[2] studied the performance of 15CrMo steel tube in high-temperature steam during the service. Effect of pre-oxidation on the steam oxidation of T92 heat-resistant steel at 650 °C was investigated by H. Xu^[3]. The steam corrosion behavior of 9Cr-0.5Mo-1.8W steel was investigated at high temperature^[4].

A crucial inducement for steel corrosion is the salinity of feed water^[5-7]. In some situations, feed water is of high quality so that the salinity could be ignored. However, in some other cases like steam injection boiler in oilfield, feed water contains kinds of salt, as the cost of feed water treatment is limited. In the operation of steam injection boiler, lots of saline feed water is injected into the reservoir to maintain high pressure and to enhance the oil extraction efficiency. Sodium sulfate (Na_2SO_4) is the most abundant salt in the feed water of steam injection boiler in Shengli Oilfield, Dongying, China. The solubility of sodium sulfate in water decreases with temperature. Therefore, during the operation of steam injection boiler, sodium sulfate tends to dissolve out on the inner wall of tubes, which could influence the corrosion behavior and lead to heat transfer deterioration. 20G steel is widely used in the manufacturing of steam injection boiler. In this study, the corrosion behavior of 20G steel exposed in precipitated Na_2SO_4 is investigated. The effects of heating time and temperature are discussed in detail.

The purpose of the study is to figure out the corrosion behavior of 20G exposed in precipitated sodium sulfate. The study has fundamental value to boiler steel performance. It is also a precondition of the research on heat transfer performance of corroded boiler tube, which has a crucial effect on safety and efficiency problems of boilers in the field of energy application.

2. EXPERIMENT DETAILS

The test samples used in experiments are made of 20G steel. The thickness of each flake is 1.5 mm. The surface is polished orderly by 280# and 320# SiC abrasive papers. The roughness of samples is the same as that of boiler tube. After polish, the test samples are cleaned by C₂H₅OH and C₃H₆O to remove the organic impurities. The chemical composition of 20G is shown in Table 1.

Table 1 Chemical composition of studied material 20G steel (wt.%-mass fraction)

Element	C	Si	Mn	S	P	Fe
Concentration	0.17-0.24	0.17-0.37	0.50-0.60	0.03	0.03	Balance

Subsequently, the sample is put into the autoclave, in which experiments are implemented. The inner wall of the autoclave is made of Hastelloy C276. The chemical properties of Hastelloy's are stable enough under the experimental conditions. Its good properties make it possible to keep samples from pollution as far as possible

during the experiments. Deionized water would be added into the autoclave to maintain the saturated condition, where saturated water and saturated steam coexist. The atmosphere around samples consists of saturated steam.

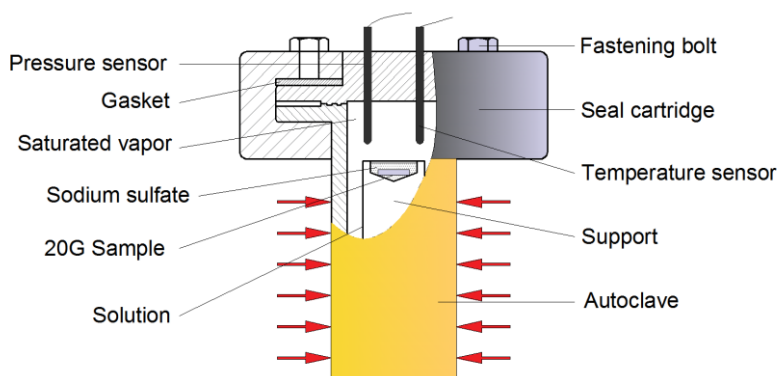


Fig.1 Experiment System

3. RESULTS AND DISCUSSION

3.1 The effect of time on corrosion behavior

The corroded surfaces are compared with original surface. The effect of heating time on corrosion behavior is studied in this section. SEM image and corresponding EDS analysis result of original sample are presented in Fig.2 and Table 2.

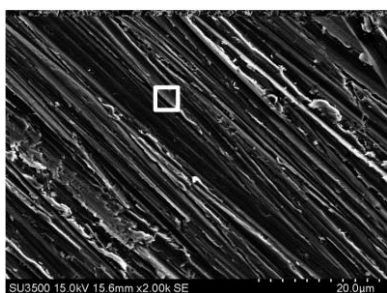


Fig.2 SEM analysis of original surface

The experiment temperature is $T = 340\text{ }^{\circ}\text{C}$. The heating time in the experiments is set as $t = 24\text{ h}$, 48 h and 72 h . As could be seen in Table 2, the mass fraction of Fe element on original surface is 92.57%, which is the most abundant element on the surface. Besides, O element could not be detected. The scratches led by polishing could be observed clearly as shown in Fig.2. The result indicates that no oxides exist on the original surface.

Table 2 EDS analysis of original sample

Element	Concentration	k ratio	wt%
C	0.73	0.00731	6.72
Si	0.05	0.00043	0.21
Mn	0.30	0.00302	0.50
Fe	57.16	0.57164	92.57

The SEM images of samples corroded in different heating time is listed in Fig.3. The corresponding EDS analysis results is summarized in Fig.4. In Fig.3 (a), many small units whose surface is smooth and amorphous could be observed as pointed by red circles. This is the primary microstructure of ferrosferric oxide Fe_3O_4 crystal, among which are many other particles. In Fig.3 (b), amorphous forms disappear, instead, octahedron-shaped form is generated as marked by yellow circles. In Fig.3 (c), the structure of octahedron-shaped form could not be observed obviously although there is still a small

quantity of octahedron existing. Instead, the surface is covered by many small particles, which is distributed homogeneously. This is a typical form of hydroxyl oxidize iron (FeOOH). FeOOH is one of the most common corrosion products of steel^[8, 9]. Therefore, it could be reasonably assumed that Fe_3O_4 is form in amorphous forms in the beginning. When the heating time $t = 48$ h, amorphous forms of Fe_3O_4 is fully developed into crystal as octahedron-shaped form. As time goes on, FeOOH is generated and accumulated gradually.

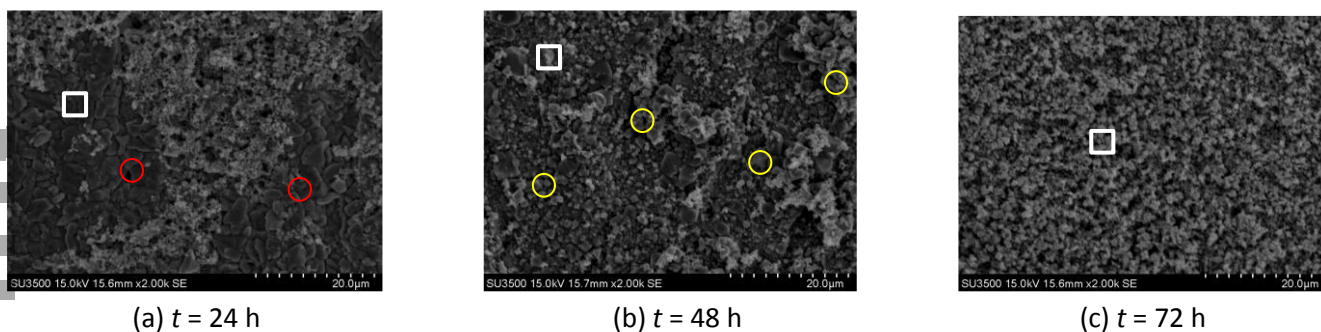


Fig.3 SEM analysis of corroded surface in different heating time

In Fig.4, it could be seen that the mass fraction of Fe element increases with time from $t = 24$ h to $t = 72$ h, while that of O elements decreased. The mass fractions of Fe element on three corroded surfaces are 86.85%, 80.80% and 75.74% respectively. The mass fractions of O element on three corroded surfaces are 12.35%, 17.72% and 22.89%. The mass fraction of Fe element in Fe_3O_4 is 72.4% while that in FeOOH is 62.9%. Qualitatively, the generation of FeOOH could lead to the decrease of Fe mass fraction. To some extent, the results prove the assumption that the variation of Fe element comes from the generation of FeOOH .

exposed in precipitated sodium sulfate under high temperature/pressure for 24 hours is investigated. The two experiment temperatures are set as $310^\circ\text{C}/9.86$ MPa and $340^\circ\text{C}/14.6$ MPa. The SEM images are shown in Fig.5. Table 3 is the corresponding EDS analysis result. As could be seen in Fig.5, more regular structures could be found in Fig.5 (b) compared with Fig.5 (a). The result indicates that more crystal substances cover the surface in Fig.5 (b).

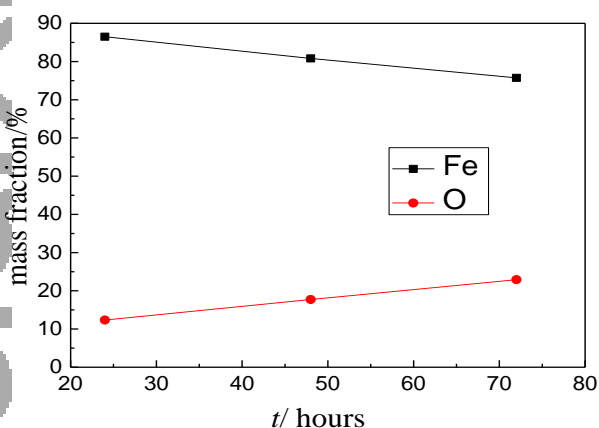


Fig.4 EDS analysis results at $T = 340^\circ\text{C}$ in different heating time

3.2 The effect of temperature on corrosion behavior

In this part, the corrosion characteristic of samples

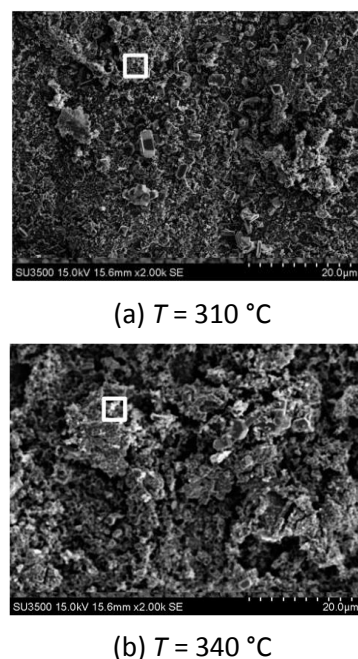


Fig.5 SEM images of corrosion surface ($t = 24$ h)

Table 3 EDS analysis of corrosion surface at different temperature ($t = 24$ h)

Element	Concentration		k ratio		wt %	
	310 °C	340 °C	310 °C	340 °C	310 °C	340 °C
C	1.45	1.16	0.01447	0.01164	1.09	0.87
O	93.51	93.26	0.31466	0.31383	14.83	14.68
S	2.46	4.11	0.02120	0.03544	0.92	1.51
Fe	192.84	194.33	1.92839	1.94328	83.17	82.93

The XRD patterns of corroded surface ($t = 24$ h, $T = 310$ °C and $T = 340$ °C) are exhibited in Fig.6. The number of peaks on spectral line at $T = 340$ °C is more than that at $T = 310$ °C. It is clear that the crystals of oxides are better developed when heating temperature $T = 340$ °C. This phenomenon further demonstrates that the crystal structure of iron oxide would be easier to be generated under higher temperature.

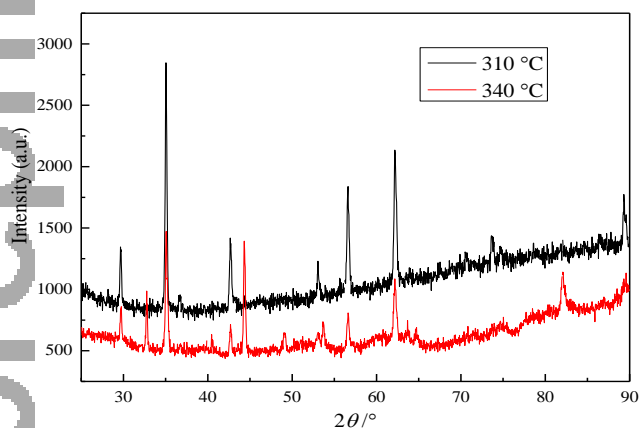


Fig.6 XRD patterns in 24 h at different temperature.

4. CONCLUSION

The corrosion behaviors of 20G corroded surface, exposed in precipitated sodium sulfate at different temperature for different heating time, are studied by a setup. The following conclusion could be drawn.

1. FeOOH and Fe₃O₄ are included in the main corrosion products under experimental conditions. As heating time changes from 24 h to 72 h, more FeOOH would be formed. Comparatively, the amount of Fe₃O₄ decreases.

2. As time goes on, FeOOH would be generated and distributed evenly on the corroded surface.

3. In the range of experimental temperature, it is easier for the crystal structures of iron oxide like FeOOH to be generated under higher temperature and higher pressure.

REFERENCE

- [1] Badovinac IJ, Piltaver IK, Peter R, Saric I, Petravic M. Formation of oxides on CoCrMo surfaces at room temperature: An XPS study. APPL SURF SCI 2019;471:475-481.
- [2] Yuan C, Hu ZF, Wu XM. Microstructure features of steam oxidation layer on 15CrMo steel tubes. HEAT TREAT METAL 2012;37:136-139.
- [3] Xu H, Liang ZY, Ding JL, Zhao QX, Guan SP. Processes, Effect of Pre-Oxidation on the Steam Oxidation of Heat-Resistant Steel T92. HIGH TEMP MATER PROCESS 2018;37:733-739.
- [4] Ishitsuka T, Inoue Y, Ogawa H. Effect of Silicon on the Steam Oxidation Resistance of a 9%Cr Heat Resistant Steel. OXIDAT METAL 2004;61:125-142.
- [5] Azar MMK, Gugtaped HS, Rezaei M. Evaluation of corrosion protection performance of electroplated zinc and zinc-graphene oxide nanocomposite coatings in air saturated 3.5 wt. % NaCl solution, COLLOID SURFACE A 2020;601:125051.
- [6] Lu CW, Lu YS, Lai ZH, Yen HW, Lee YL, Comparative corrosion behavior of Fe₅₀Mn₃₀Co₁₀Cr₁₀ dual-phase high-entropy alloy and CoCrFeMnNi high-entropy alloy in 3.5 wt% NaCl solution, J ALLOYS COMPOUNDS 2020; 842:155824.
- [7] Onyeachu IB, Solomon MM. Benzotriazole derivative as an effective corrosion inhibitor for low carbon steel in 1 M HCl and 1 M HCl+3.5 wt% NaCl solutions. J MOL LIQ 2020;313:113536.
- [8] Song LY, Chen ZY. Effect of gamma-FeOOH and gamma-Fe₂O₃ on the Corrosion of Q235 Carbon Steel under Visible Light, J ELECTROCHEM SOC 2015;162:C79-C84.
- [9] Luo HQ, Tao KY, Gong Y, K-doped FeOOH/Fe₃O₄ nanoparticles grown on a stainless steel substrate with superior and increasing specific capacity, DALTON TRANS 2019;48:2491-2504.